Online Detection and Estimation of Grid Impedance Variation for Distributed Power Generation

Jebali-Ben Ghorbal, Manel; Ghzaiel, Walid; Slama-Belkhodja, Ilhem; Guerrero, Josep M.

Published in:
Proceedings of the 16th IEEE Mediterranean Electrotechnical Conference (MELECON), 2012

DOI (link to publication from Publisher):
10.1109/MELCON.2012.6196495

Publication date:
2012

Document Version
Early version, also known as pre-print

Online Detection and Estimation of Grid Impedance Variation for Distributed Power Generation

Manel Jebali-Ben Ghorbal*, Walid Ghzaiel†, Ilhem Slama-Belkhodja‡ and Josep M. Guerrero§
*†‡University of Tunis El Manar, ENIT-L.S.E, BP 37-1002, Tunis le Belvédère, Tunisie
* Email: maneljebali2001@yahoo.fr, †Email: ghzaiel.walid@gmail.com, ‡Email:ilhem.slama@enit.rnu.tn
§ Dept. Energy Technology, Aalborg University, 9220 Aalborg, Denmark
Technical University of Catalonia, 08036 Barcelona, Spain, Email:joz@et.aau.dk

***Abstract*—A better knowledge of the grid impedance is essential in order to improve power quality and control of the Distributed Power Generation Systems (DPGS) and also for a safe connection or reconnection to the utility grid. An LCL-filter associated to a Voltage Source Inverter (VSI) is usually used in DPGS based on renewable energy. The VSI controller is used to determine the grid impedance in both healthy operation and faulty modes. When grid faults occurence, the grid impedance variations have a considerable influence on the control and the stability of the system, even on the decision to disconnect the DPG systems of the network. This work presents a rapid and simple technique to detect the grid impedance variation and to determine the grid impedance before and after grid faults accurs. Implementation on FPGA control board, simulations and experimental results are presented to validate the described method.**

I. Introduction

The Distributed Power Generation Systems (DPGS) are gaining popularity due to their contribution to feed the grid with renewable energy. They need smart interfaces between the operator and the network to improve power quality and to satisfy the costumers need in energy. This is the reason why grid information is of primer importance when connecting the DG system to the utility network. Indeed, a grid impedance variation has an effect on the stability of the system [1], and on the current control loop of a Voltage Source Inverter (VSI) [2]. The grid impedance information can also detect a grid failure and be useful to prevent the DG from other complications such as the islanding operation. In the litterature,several methods were discussed, for grid impedance variation detection or grid impedance estimation [3], [4], [5]. These methods can be classified into three categories:

- Methods using control loop variations to estimate resistive and inductive parts of the grid impedance to include them into the control to improve its performances [6].
- Methods using harmonic injection signal into the system, then use mathematical methods to analyse the output signal in order to determine the grid impedance [7], [9], [12], and [13].
- Methods using extra devices for the grid impedance estimation purpose [8].

In previous studies focusing on grid impedance calculation methods using inter-harmonic injection signal, the grid parameters are extracted from current and voltage responses at the point of common coupling (PCC). These methods complied with hardware limitations and have the real advantage to be embeded in a PV-inverter platform. However, to obtain a good accuracy, the best knowledge of the background environment is required, in order to substract background voltage noises from the obtained voltage response. For this purpose, dedicated A/D hardware devices and sensible sensors are required [14]. Another work in the same field investigated an inter-harmonic voltage injection within the digital processor instead of the grid voltage [2]. The main drawback of this method is that the disturbance, repetitive or not, should be carefully chosen in terms of amplitude, duration and frequency to avoid negative effect on the THD of the grid. Another method described in [15] discussed the variation of the inductive part of the grid impedance L_g on the current controller, and proposed an L_g estimator by exciting the LCL-filter. However, this method did not take into consideration the resistive part of the grid R_g.

The method presented in this paper is from the first group of classification methods. Its principle consists on detecting fault occurence using temporal redundancies of current measurements, and then estimating the impedance variation by leading the system to resonance. To avoid resonance and its negative effect, the algorithm is stopped as soon as the resonance is reached from one hand, and from the other hand a passive damping is used to achieve the stability of system and to reduce the effect of resonance phenomenon. Note that there are two damping methods: passive damping consisting on adding a resistor in series with the LCL-filter capacitance and active damping which is carried out by implementing a virtual resistor in the control strategy in order to avoid reducing the effeciency of system.

II. Principle of the proposed method

A. Studied system

The studied system topology is shown in Fig. 1. The grid is connected to a pulsewidth-modulation (PWM) Voltage-Source Inverter (VSI) with a low-pass LCL-filter and the grid is presented by a single phase sinusoidal voltage source with an impedance Z_g. The impedance of the grid incorporates a resistive part R_g and an inductive part L_g. The LCL-filter is choosen especially due to its ability to operate as well in islanded mode as in grid connected mode which is a significant advantage for DPGS applications. Besides, as with L-filter, high frequency current harmonics can be limited with the use

of the LCL-filter. The main issue to be taken into account when adopting the LCL-filter solution is its resonance. It's worth to say that the grid background disturbances has a great impact on the LCL resonance frequency. Indeed, this point was investigated in the proposed method to calculate the grid inductive part of the impedance.

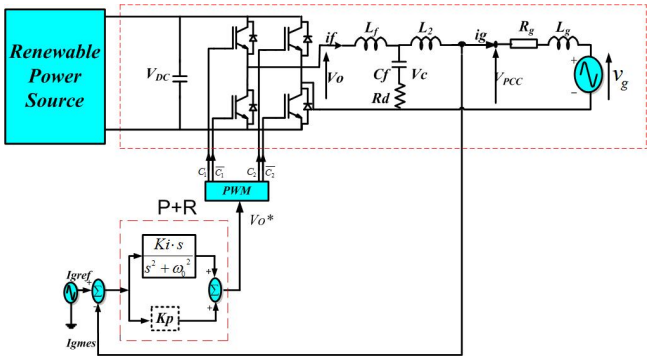

Fig. 1. Grid-connected PWM-single phase inverter.

B. Grid Impedance model and principle of the method

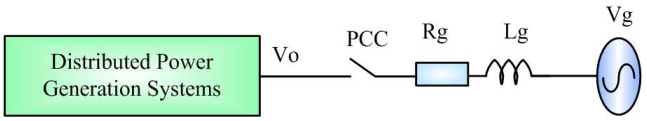

Fig. 2. Simplified grid model.

Several grid models have been proposed in the literature [10], [11]. Each model was trying to describe the grid harmonic behavior with a different level of complexity. For example, the authors in [9] considered the grid as a cascaded Z-blocks. Each block involves a resistive and inductive parts, a capacitive part which presents the consumer side of the grid and an ideal source supply denote Vs. In this work, we consider the simplest grid model, a series inductive-resistive branch as shown in Fig. 2. The total grid impedance is then $Z_g = R_g + j\omega.L_g$ and V_g is an ideal source supply. The output VSI-voltage is denoted V_o.

The principle of the method of detection and estimation of grid impedance is depicted in Fig. 3. As it is detailed in the subsection (C), the LCL-filter excitation allows the determination of the grid inductance parameter L_g, then, a residual based of current measurement is continuously caluclated. When its value becomes higer than a predefined threshold, so when a grid fault is detected, the system is driven near the resonance to perform a new caluclation of L_g parameter value. The knwoledge of L_g value and residual measurements, before and after fault occurence, allow to calculate grid resistance value R_g.

C. PR-controller design and grid impedance estimation method

First, the influence of the inductive part of the grid on the LCL filter is discussed. Fig. 4 shows the block diagram of the

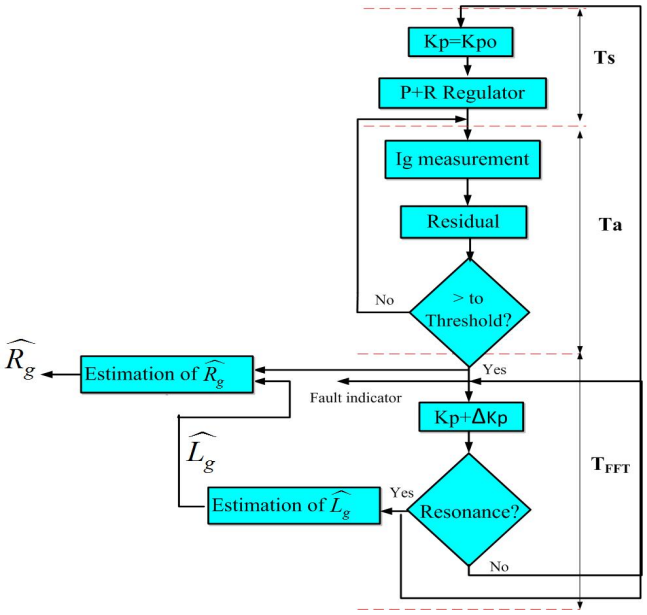

Fig. 3. Principle of the proposed method.

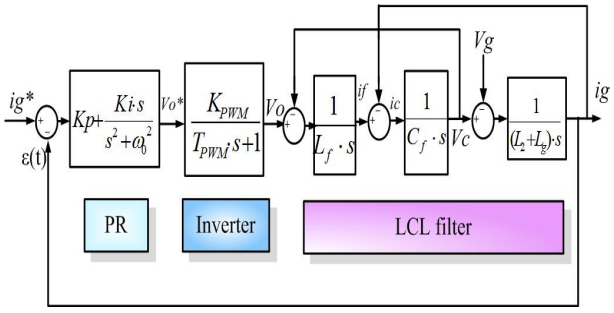

Fig. 4. Block diagram of the grid current control loop using PR.

PR regulator where s is the Laplace operator, K_{PWM} the gain of the inverter and T_{PWM} the control delay. For calculation simplifications consideration, the resistive part is neglected. The transfer function of the VSI closed loop output voltage V_o to the grid current I_g can be expressed as

$$\frac{I_g}{V_o} = \frac{1}{L_f.s} \cdot \frac{(\frac{R_d}{L_2+L_g}s + Z_f^2)}{(s^2 + \omega_{res}^2 C_f R_d s + \omega_{res}^2)} \tag{1}$$

being

$$\begin{cases} Z_f^2 = \frac{1}{C_f(L_2+L_g)} \\ \omega_{res} = \sqrt{\frac{L_f+(L_2+L_g)}{L_f.C_f.(L_2+L_g)}} \end{cases} \tag{2}$$

From (2), the expression of the resonance frequency of the LCL filter is deduced. Hence, an increase in the inductive grid part impedance leads to a decrease in the resonance frequency of the LCL-filter as is shown in Fig. 5. The resonance frequency should be of the following range

$$10\omega_g < \omega_{res} < \frac{\omega_{PWM}}{2} \tag{3}$$

being ω_g the grid frequency and ω_{PWM} the switching frequency which is usually chosen between 1Khz and 20Khz. The bode plot of the transfer function from inverter output voltage V_o to the grid current i_g (1) of Fig. 6 is drawn for two different values of L_g. A first spike is shown for $L_g = 1.5mH$ and a second one for $L_g = 4.5mH$.

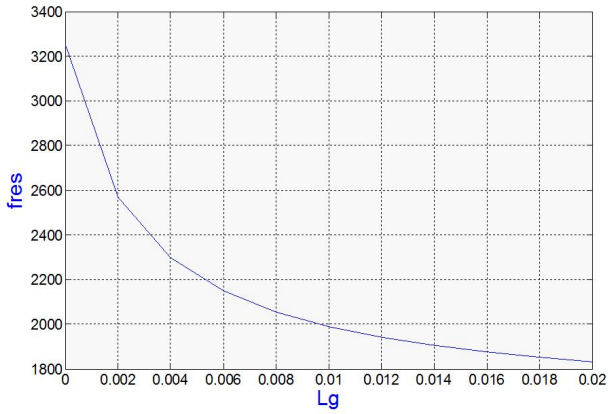

Fig. 5. Influence of L_g variations on the resonance frequency f_{res}.

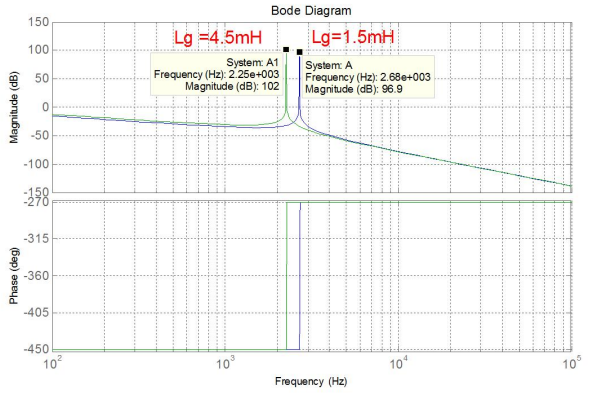

Fig. 6. Bode diagram of the transfer function of V_o to i_g

The grid impedance value is then derived from the resonance frequency of the LCL-filter expressed in (2). Several methods have been proposed for the excitation of the LCL-filter [2], [12], [15], and various types of approach are mentioned to reach the resonance. In our case, the method increases the proportional gain of the PR regulator K_p until the roots move close to the right-half plane that's to say the instability region. Fig. 7 shows the migration of these resonant poles with the increase of K_p.

As the proportional gain is incremented, the system stability margin is progressively reduced to zero. It is noticeable that every stage needs a speacial period, denoted T_{FFT}, to make it possible to calculate the Fourier Transform of the obtained current signal. Having the resonant frequency of the system, the grid inductance can be consequently deduced as follows

$$\widehat{L_g} = \frac{(L_2 + L_f) - (4\pi^2.L_f.C_f.L_2.f_{res}^2)}{(4\pi^2.L_f.C_f.f_{res}^2 - 1)} \quad (4)$$

being $\widehat{L_g}$ the estimated grid inductance.

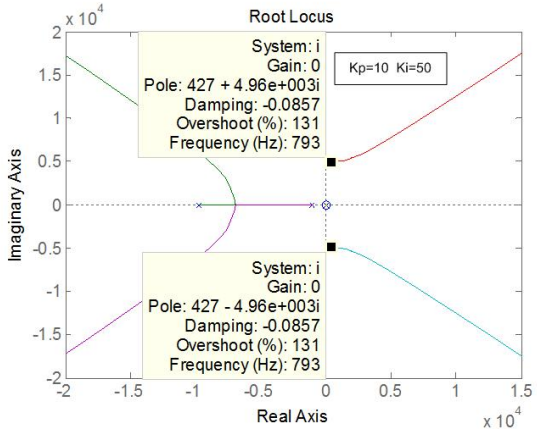

(a) Kp=10 and Ki=50

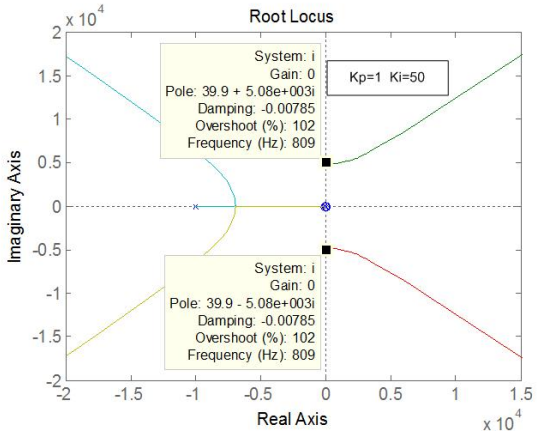

(b) Kp=1 and Ki=50

Fig. 7. Root locus of the PR-controlled system for two values of K_p

D. Grid Impedance Variation Detection Method

The method is based on the dynamic space parity approach, and more precisely on the temporal redundancies of current measurement. Theoretical developments are given in [16], and their application to fault detection and isolation (FDI) of faulty sensor in electrical drives has been experimentally demonstrated. In addition to the mathematical developments, the principle can be simply explained: in healthy conditions, with constant grid impedance, with a very low measurement sampling time, T_a, the difference between two consecutive measurements remains lower than a calculated threshold.

When a grid impedance variation occurs, this difference increases and the defined residual becomes higher than the threshold. The residual Res_{ig_k} is defined by (5) and (6).

$$Res_{ig_k} = r_k + r_{k-1} + r_{k-2} \tag{5}$$

$$r_k = |i_{g_k} - 2i_{g_{k-1}} + i_{g_{k-2}}| \tag{6}$$

where i_{g_k}, $i_{g_{k-1}}$, $i_{g_{k-2}}$ are the measured current at kT_a, $(k-1)T_a$ and $(k-2)T_a$ respectively.

As the measured current waveform is sinusoidal, an analytical expression of the maximum value of Res_{ig_k} is performed [16] and leads to the threshold expressed by (7).

$$\begin{cases} \varepsilon = 3\omega^2 T_a^2 I_m \\ I_m = \frac{V_{o_m} - V_{g_m}}{|Z_g|} \end{cases} \tag{7}$$

with $\omega = \frac{2\pi}{\tau_s}$, τ_s is the system time constant, V_{o_m} the maximum VSI output voltage, V_{g_m} the maximum grid voltage and $|Z_g|$ is the grid impedance amplitude. As L_g was estimated as explained before, R_g can be deduced using (7) as follows:

$$\widehat{R_g} = \sqrt{\frac{9\omega^4 T_a^4}{\varepsilon^2}(V_{o_m} - V_{g_m})^2 - (\omega L_g)^2} \tag{8}$$

However, if the grid impedance increases or decreases, the current residual measurement Res_{Ig} changes. As the residual value in healthy mode is denoted by ε_h and by ε_f in faulty mode, the grid impedance variation is calculated as shown in (10).

$$|\Delta Z| = \frac{k_f}{\varepsilon_f} - \frac{k_h}{\varepsilon_h} \tag{9}$$

$$\begin{cases} |\Delta Z| = 3\omega^2 T_a^2 (E_m - V_{g_m})(\frac{1}{\varepsilon_f} - \frac{1}{\varepsilon_h}) \\ |\Delta Z| = |Z_f| - |Z_h| \end{cases} \tag{10}$$

III. Simulations Results

Simulations were carried out using Matlab and PSIM softwares. The method described above for detection and estimation of grid impedance variation is tested on a $2.5kW$ single phase inverter. The system's parameters are given in table I. The grid resistance R_g is set to 0.673Ω and the L_g to $1.5mH$. The variation of the grid impedance Z_g is simulated by inserting a variable fault impedance $Z_d = R_d + j\omega L_d$, controlled by a switching gate block. For more clarity, in healthy mode, the grid impedance variation is null ($Z_d = 0$) so the total grid impedance is equal to Z_{g1}. Then, as the switch gate is opened, at the fault instant, the grid impedance varies according to (11). Fig. 8 presents the grid current evolution as the incrementation of k_p is proceeding from 17 to 31. The figure shows the tendency of the system to be unstable as the current i_g increased gradually until reaching the resonance. As can be seen, the residual value exceeds its threshold as the resonance phenemona occurs, and presents a peak at the instant of fault, i.e at $0.53s$.

$$Z_g = Z_{g1} + Z_d \tag{11}$$

TABLE I
System Parameters

Parameter and designation	value
Inverter nominal power P_N	2.5 kW
Filter inductance L_f	6mH
Filter inductance L_2	2mH
Filter capacitance C_f	1.6μH
Power widht modulation switching frequency f_{PWM}	16kHz
DC voltage bus V_{DC}	450V
Grid voltage V_g	230V
Inverter gain K_{PWM}	1
Acquisition Time T_a	$5\mu s$

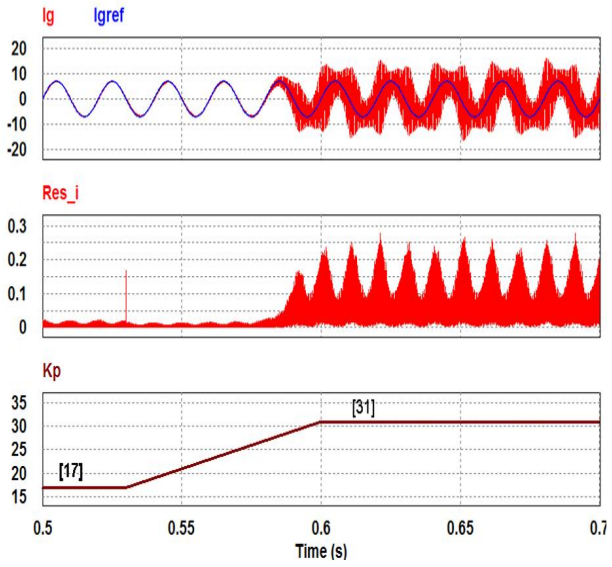

Fig. 8. LCL-Resonance phenomenon of the grid current i_g by the incrementation of k_p (fault instant $T_f = 0.53s$).

Fig.9(a) and Fig.9(b) show the grid current residual measurement for two different values of Z_d. In these figures, the residual amplitude increases according the the grid impedance variation. Nevertheless, it remains so high comparing with its value in healthy mode. The details in Fig. 10 shows the similarity between theory and simulations. The acquisition time for simulation is chosen equal to $5\mu s$ and the residual signal lasts $4T_a = 20\mu s$ as explained in [16]. After detecting a grid fault occurance, a Fast Fourier Transformation can be done in order to determine the resonance frequency f_{res}. Fig. 11(a) and Fig. 11(b) shows the measured grid current FFT for two grid impedance values. In fact, in Fig. 11(a), there is no grid impedance variation, so the total grid inductance is equal to Z_{g_1}. However, in Fig. 11(b), the grid impedance increases to $3Z_{g_1}$ (11). Table II gives the error of R_g and for L_g for diffrent values of grid impedance with different $\frac{X}{R}$.

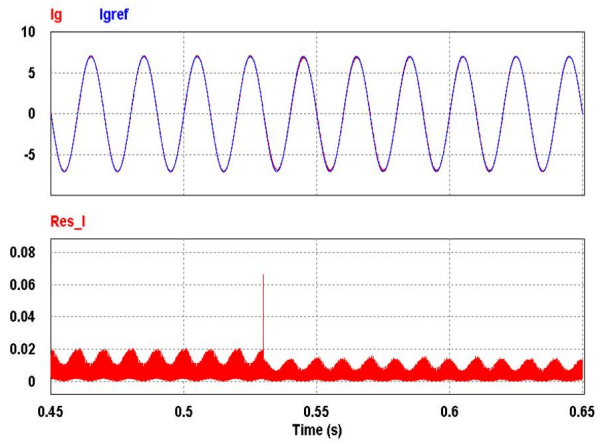

(a) $\{R_{g_1}, L_{g_1}\} = \{0.673\Omega, 1.5mH\}$ and $Z_d = Z_{g_1}$

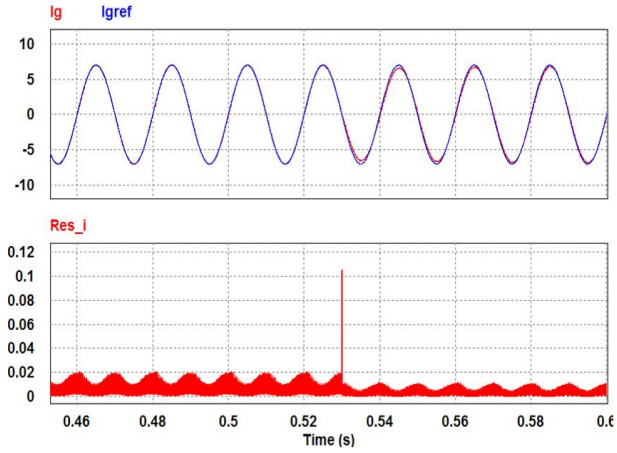

(b) $\{R_{g_1}, L_{g_1}\} = \{0.673\Omega, 1.5mH\}$ and $Z_d = 2Z_{g_1}$

Fig. 9. Residual measurement of the grid current with Z_g variation at $0.53s$

TABLE II
ERROR OF THE PROPOSED GRID IMPEDANCE ESTIMATION METHOD

$\frac{X}{R} ratio$	Real L_g value	Estimated L_g value	Error of L_g in %
0.13	1.5 mH	1.44 mH	4
0.13	4.5 mH	4.40 mH	2.22
0.7	1.5 mH	1.47 mH	1.33
0.7	4.5 mH	4.42 mH	1.77
1.17	1.5 mH	1.47 mH	1.33
1.17	4.5 mH	4.47 mH	0.66

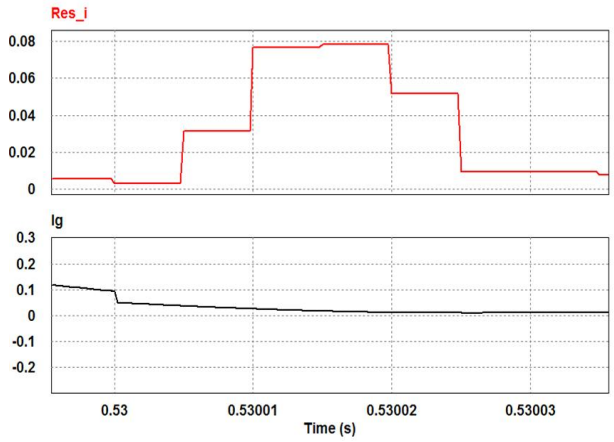

Fig. 10. Details of Fig.9 (b)

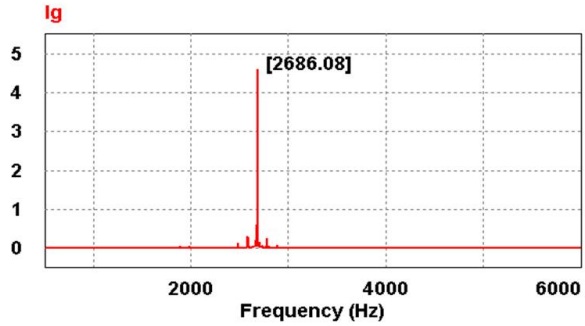

(a) FFT analysis before grid grid impedance variation $(Z_d = 0)$

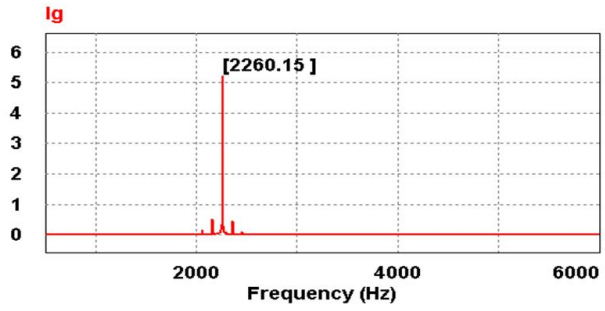

(b) Grid current FFT analysis after grid impedance variation $(Z_d = Z_{g_1})$

Fig. 11. FFT analysis for i_g with $R_{g_1} = 0.673\Omega$ and $L_{g_1} = 1.5mH$

IV. EXPERIMENTAL RESULTS

The method of a grid impedance variation was tested on a three-phase-1.5kW Induction Machine. The FPGA target device used is Xilinx SPARTAN3 XCS400PQ208. It has 400.000 logical gates and a 50-MHz oscillator ($20ns$ clock period).One of the three phase-current of the IM was measured using hall-effect sensors (LEM 25NA). An interface board (ARCU3I)allows the voltage level adaptation between the LEMs sensors and the ADC interface (2.5V/20A). An Anolog-Digital 12-bit-circuit (AD9221) is used for AD conversion of measured stator current, the computation time of the acquisition module is about $2.4\mu s$. A 10-bits Digital-Analog (DA) converter circuit allowed viewing the current residual

measurement on a scope. In Fig. 12, experimental results of the current residual after a perturbation are shown. The perturbation was set in the FPGA program of the residual calculation. As the variation of the impedance occurs, the level of the residual measurement. increases and presents a franc spike. The details in Fig. 13 depict the wave form of the residual taht perfectly match with the simulation results. The acquisition time is set to $100\mu s$ which is higher than the real acquisition time but it allowed a good residual viewing on the scope. Experimental results are similar to simulations and demonstrate the effectiveness of the proposed method.

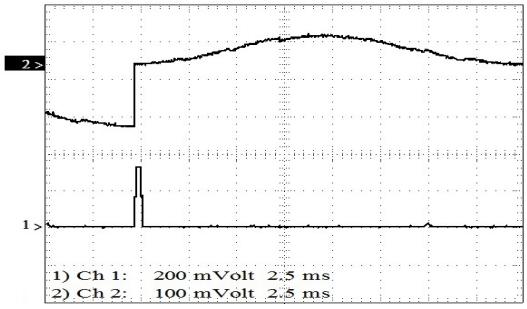

Fig. 12. Experimental result of the residual measurement of the current

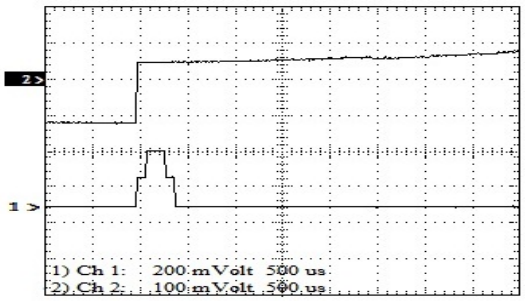

Fig. 13. Details of Fig. 12

V. Conclusion

A novel technique for online dection and estimation of grid impedance variation is presented. A PR-controller for a grid connected LCL-filter inverter is proposed. Simulations demonstrate the reliability of the method, due to the fact that it can be easily implemented and it respects the experimental background limitations. The main features of this method is that it gives accurate values of the impedance of the grid in both safe and faulty modes and can operate without network utility interruption in weak grid system. The error of the estimated inductive part of the grid is low enough to consider the method satisfactory.

Acknowledgment

This work was supported by the Tunisian Ministry of High Education and Research under Grant LSE-ENIT-LR 11ES15. The authors would like also to acknowledge the contributions to this project: A1/048431/11.

References

[1] S. Yang, Q. Lei, F.Z. Peng, Z. Qian, " A Robust Control Scheme for Grid-Connected Voltage-Source Inverters, " *IEEE transactions on Industrial Electronics,*. Vol.58, no. 1 , pp.202 -212,Jan. 2011.

[2] Guoqiao Shen,Jun Zhang,Xiao Li,Chengrui Du,Dehong Xu, " Current control optimization for grid-tied inverters with grid impedance estimation, " *2010 Twenty-Fifth Annual IEEE Applied Power Electronics Conference and Exposition (APEC),* pp.861-866, Feb. 2010.

[3] A. Moallem, D. Yazdani, A. Bakhshai, P. Jain, "Frequency domain identification of the utility grid parameters for distributed power generation systems, " *2011 Twenty-Sixth Annual IEEE Applied Power Electronics Conference and Exposition (APEC),* pp.965-969,Mar. 2011.

[4] H. Geng, D. Xu, B. Wu, G. Yang, " Active Islanding Detection for Inverter-Based Distributed Generation Systems With Power Control Interface, " *IEEE Transactions on Energy Conversion,* Vol.26, no.4, pp.1063-1072, Jul. 2011.

[5] R. Schulze, P. Schegner, ; R. Zivanovic, " Parameter Identification of Unsymmetrical Transmission Lines Using Fault Records Obtained From Protective Relays, " *IEEE Transactions on Power Delivery,* Vol.26, no. 2 ,pp.1265-1272, Apr. 2011.

[6] A.V. Timbus, P. Rodriguez, R. Teodorescu, M. Ciobotaru, "Line Impedance Estimation Using Active and Reactive Power Variations," *IEEE, Power Electronics Specialists Conference, 2007. PESC 2007.* pp.1273 - 1279, Jun. 2007.

[7] A.V. Timbus,R. Teodorescu, F. Blaabjerg, U. Borup, " Online grid measurement and ENS detection for PV inverter running on highly inductive grid, " *IEEE Power Electronics Letters,* Vol.2, no. 3, pp. 77 - 82, Sept. 2004.

[8] Z. Suquan, Z. Liying, Z. Yanjun, X. Yan, L. Guihua, L. Bijun, L. Lei, G. Chengming, " A New Approach to Branch Parameter Estimation of Power Grid Based on PMU Connected to the Grid Through an LCL Filter, " *2011 Asia-Pacific Power and Energy Engineering Conference (APPEEC),* pp.1-5, Mar. 2011.

[9] L. Asiminoaei, R. Teodorescu, F. Blaabjerg, U. Borup, " A new method of on-line grid impedance estimation for PV inverter, " *Nineteenth Annual IEEE Applied Power Electronics Conference and Exposition, 2004. APEC '04,* Vol.3, pp.1527-1533, Sep. 2004.

[10] M. Mata-Dumenjo, J. Sanchez-Navarro, M. Rossetti, A. Junyent-Ferre, O. Gomis-Bellmunt, " Integrated Simulation of a Doubly fed induction generator wind turbine, " *13th European Conference on Power Electronics and Applications, 2009. EPE '09,* Vol.3, pp.1-7, Sept. 2009.

[11] A. Tarkiainen, R. Pollanen, M. Niemela, J. Pyrhonen, " Identification of grid impedance for purposes of voltage feedback active filtering, " *IEEE Power Electronics Letters,* Vol.2, no. 1, pp. 6-10, Mar. 2004.

[12] L. Asiminoaei, R. Teodorescu, F. Blaabjerg, U. Borup, " A digital controlled PV-inverter with grid impedance estimation for ENS detection, " *IEEE Transactions on Power Electronics,* Vol.20, no. 6 ,pp. 1480 - 1490, Nov. 2005.

[13] L. Asiminoaei, R. Teodorescu, F. Blaabjerg, U. Borup, " Implementation and Test of an Online Embedded Grid Impedance Estimation Technique for PV Inverters, " *IEEE Transactions on Industrial Electronics,* Vol.52, no. 4 ,pp. 1136-1144, Aug. 2005.

[14] B. Palethorpe, M. Sumner, D.W.P. Thomas, "Power system impedance measurement using a power electronic converter, " *IEEE Power Electronics Letters,* Vol.43, no. 5, pp. 1401-1407, Oct. 2007.

[15] M. Liserre, F. Blaabjerg, R. Teodorescu, "Grid Impedance Estimation via Excitation of LCL -Filter Resonance, " *Proc. on Harmonics and Quality of Power, 2000,* Vol.1, pp. 208-213 , 2000.

[16] H. Berriri, M.W. Naouar, I. Slama-Belkhodja, "Easy and Fast Sensor Fault Detection and Isolation Algorithm for Electrical Drives, " *IEEE Transactions on Power Electronics,* Vol.27, no. 2, pp.490-499, Apr. 2011.